

# Impacts of Black-Hole-Forming Supernova Explosions on the Diffuse Neutrino Background

KEN'ICHIRO NAKAZATO <sup>1</sup>, RYUICHIRO AKAHO <sup>2</sup>, YOSUKE ASHIDA <sup>3</sup>, AND TAKUJI TSUJIMOTO <sup>4</sup>

<sup>1</sup>*Faculty of Arts and Science, Kyushu University, Fukuoka 819-0395, Japan*

<sup>2</sup>*Faculty of Science and Engineering, Waseda University, Tokyo 169-8555, Japan*

<sup>3</sup>*Department of Physics and Astronomy, University of Utah, Salt Lake City, UT 84112, USA*

<sup>4</sup>*National Astronomical Observatory of Japan, Mitaka, Tokyo 181-8588, Japan*

## ABSTRACT

Flux spectrum, event rate, and experimental sensitivity are investigated for the diffuse supernova neutrino background (DSNB), which is originated from past stellar collapses and also known as supernova relic neutrino background. For this purpose, the contribution of collapses that lead to successful supernova (SN) explosion and black hole (BH) formation simultaneously, which are suggested to be a non-negligible population from the perspective of Galactic chemical evolution, is taken into account. If the BH-forming SNe involve the matter fallback onto the protoneutron star for the long term, their total emitted neutrino energy becomes much larger than that of ordinary SNe and failed SNe (BH formation without explosion). The expected event rate according to the current DSNB model is enhanced by up to a factor of two due to the BH-forming SNe, depending on their fraction and the neutrino mass hierarchy. In any case, the operation time required to detect the DSNB at Hyper-Kamiokande would be reduced by such contribution.

*Keywords:* Neutrino astronomy (1100) — Supernova neutrinos (1666) — Core-collapse supernovae (304) — Massive stars (732) — Neutron stars (1108) — Black holes (162) — Galaxy chemical evolution (580)

## 1. INTRODUCTION

Supernova (SN) explosions supply the elements synthesized inside stars, serving as the building blocks for the next generation of stars, planets, and life. Understanding the properties of progenitors and explosion mechanisms of SNe is crucial for unraveling the history of the Universe. In particular for the study of core-collapse SNe, neutrinos are expected to be a powerful tool. Stars with masses larger than  $\sim 8M_{\odot}$  experience core collapse at the end of their evolution, leading to the emission of a huge amount of neutrinos. In fact, neutrinos from SN1987A, which is a core-collapse SN appeared in the Large Magellanic Cloud, were successfully detected (Hirata et al. 1987; Bionta et al. 1987; Alekseev et al. 1987). In case that a next Galactic SN occurs, currently operating neutrino detectors, such as Super-Kamiokande (SK), are expected to detect statistically sufficient number of neutrino events (e.g., Abbasi et al. 2011; Abe et al. 2016; Kashiwagi et al. 2024) and various insights into SN explosions will be derived from the neutrino observations (Abe et al. 2021a; Suwa et al.

2022, 2024; Nagakura & Vartanyan 2022; Harada et al. 2023a).

Another approach to detecting neutrinos from SNe is to concentrate on the cosmic background. Neutrinos from distant SNe have been accumulated to form the diffuse SN neutrino background (DSNB), or SN relic neutrino (SRN) background. The upper bounds on the  $\bar{\nu}_e$  flux have been provided by detectors such as SK (Bays et al. 2012; Zhang et al. 2015; Abe et al. 2021b), KamLAND (Gando et al. 2012; Abe et al. 2022), and SK-Gd (Harada et al. 2023b), which is the SK experiment with gadolinium-loaded water (Beacom & Vagins 2004). Furthermore, a larger-volume water Cherenkov detector, Hyper-Kamiokande (HK), is currently under construction (Abe et al. 2018), and other types of detectors such as liquid scintillators and argon/xenon-based detectors are planned. Predictions of the DSNB detection are exhibited for these future detectors including JUNO and DUNE (Priya & Lunardini 2017; Møller et al. 2018; Sawatzki et al. 2021; Li et al. 2022; Suliga et al. 2022).

Theoretical estimations of the DSNB flux and predictions of the event rates have been investigated for a long time (Bisnovaty-Kogan & Seidov 1982; Krauss

et al. 1984; Dar 1985). Since models of DSNB involve a wide range of physical and astrophysical factors, improvements to the model have been made in many aspects. The spectrum of neutrinos emitted from a core-collapse SN depends on the progenitor, particularly its initial mass and metallicity. For estimating the DSNB flux, the average spectrum weighted by the initial mass function (IMF) is often used (Totani & Sato 1995), and a large sample of progenitor models is currently under consideration (Horiuchi et al. 2018; Kresse et al. 2021). The variation of IMF is also being discussed (Ziegler et al. 2022; Aoyama et al. 2023; Ashida et al. 2023). The evolution of progenitors may be affected by binary interactions (Horiuchi et al. 2021). The cosmic SN rate, or star formation history, is deduced from astronomical observations (Totani et al. 1996; Hartmann & Woosley 1997; Malaney 1997; Kaplinghat et al. 2000; Horiuchi et al. 2009; Mathews et al. 2014) and the cosmic chemical evolution contributes to the metallicity distribution of progenitors (Nakazato et al. 2015). The emission of neutrinos from SNe itself involves uncertainty, particularly in the late phase (Nakazato 2013; Ashida & Nakazato 2022; Ekanger et al. 2022, 2024). Flavor mixing caused by neutrino oscillations is a factor that influences the event rates of DSNB (Ando et al. 2003; Galais et al. 2010), and the effects of exotic physics in the neutrino sector are also being investigated (Ando 2003; Fogli et al. 2004; de Gouvêa et al. 2020, 2022; Tabrizi & Horiuchi 2021; Iváñez-Ballesteros & Volpe 2023). Furthermore, the DSNB flux may be related to other cosmic background radiation such as MeV gamma rays (Strigari et al. 2005; Anandagoda et al. 2023) and non-thermal high-energy neutrinos (Ashida 2024). Incidentally, neutrinos emitted from accretion disks formed around SNe may contribute to the cosmic background radiation (Schilbach et al. 2019; Wei et al. 2024). The basics of DSNB are covered in several previous reviews. (Ando & Sato 2004; Beacom 2010; Lunardini 2016; Mathews et al. 2020; Ando et al. 2023).

In the present paper, we focus on the stellar core collapses which lead to black hole (BH) formation. Neutrinos are emitted from the BH-forming collapse, as well as the ordinary core-collapse SNe, and these neutrinos are in the same energy regime as the DSNB (Iocco et al. 2005; Nakazato et al. 2006; Lunardini 2009). In previous studies on the DSNB, two scenarios for the core collapse of massive stars are considered: those resulting in an ordinary SN explosion, leaving a neutron star (NS), and those leading to BH formation without an explosion, which are known as failed SNe. This limitation on the scenario of core collapse makes sense because, according to numerical studies, successful explosions that

make BHs are predicted as a relatively rare event (see Fig. 13 of Sukhbold et al. 2016). Recently, however, the examples for this case are investigated in detail (e.g., Burrows et al. 2023). Furthermore, some astronomical phenomena such as GRB 980425/SN1998bw (Iwamoto et al. 1998) and W50/SS 433 (Poutanen et al. 2007) are likely to be associated with core-collapse SNe that result in the formation of BHs. Hereafter, we refer to this subset as BH-forming SNe.

The perspective of nucleosynthesis implied from chemical evolution at the early Galaxy has significantly raised the importance of contribution from BH-forming SNe. This suggests two types of BH-forming SNe, each of which is implied to be a non-negligible population (e.g., Nomoto et al. 2006). First, some studies propose that core-collapse SNe with large explosion energy ( $\gtrsim 10^{52}$  erg), which are referred to as hypernovae, should promote chemical enrichment with its contributed fraction as much as 50% of massive ( $> 20 M_{\odot}$ ) stars to account for the observed abundance of some heavy elements including Zn among Galactic halo stars (Kobayashi et al. 2006, 2020). These hypernovae are generally considered to be BH-forming SNe that generate a jet-like explosion powered by energy from the rotating BH. In addition, hypernovae could play a key role as the dominant site of  $\nu p$ -process nucleosynthesis that can account for a large portion of abundances of Mo and Ru for low-metallicity stars (Fujibayashi et al. 2015; Sasaki et al. 2022).

Another candidate of BH-forming SNe is the so-called faint SNe whose luminosity is very low due to a negligibly small ejection of synthesized  $^{56}\text{Ni}$  (e.g., Heger et al. 2003). Faint SNe have been highlighted as the origin of a subset of carbon-enhanced metal-poor (CEMP) stars in Galactic halo (Nomoto et al. 2013). An event frequency of faint SNe could be approximately inferred from the fraction of this kind of stars against halo stars, which is estimated to be 20% among stars with  $[\text{Fe}/\text{H}] \leq -2$  (Placco et al. 2014). In addition to these arguments, there is a recent report that the inclusion of contribution from faint SNe with tens of percent leads to better agreement with the observed abundance of stars in the solar neighborhood (Pignatari et al. 2023). In the end, BH-forming SNe that possibly emerge as hypernovae or faint SNe, are suggested to be a non-minor population that could be, as not an unrealistic case, counted up to a half of all core-collapse SNe.

Although the detailed explosion mechanisms and formation processes of BHs are not identified for these BH-forming SNe, they should accompany the emission of a huge amount of neutrinos as well as the ordinary core-collapse SNe and failed SNe. In this study, we in-

investigate the impact of BH-forming SNe on the DSNB flux updating our previous study (Ashida et al. 2023). This paper is organized as follows. In § 2, we describe the spectral model of neutrinos emitted from the BH-forming SNe. While the dynamics of BH-forming SNe includes uncertainties, we focus on the case induced by fallback mass accretion with a long duration. The formulation of the DSNB flux is presented in § 3. Issues concerning rates of core-collapse SNe and failed SNe based on the model of galactic chemical evolution are also provided. In § 4, we investigate the DSNB event rate of  $\bar{\nu}_e$ . Furthermore, the experimental sensitivities at HK are evaluated. Finally, a summary and discussion are provided in § 5.

## 2. NEUTRINO EMISSION FROM FALLBACK INDUCED BH FORMATION

In this section, we consider the neutrino emission from the BH-forming supernovae. Unfortunately, their dynamics is still not well understood. In particular, the time interval from the core bounce to BH formation, which corresponds to the duration of the neutrino emission, has notable impacts; generally the total energy of emitted neutrinos gets larger for a longer duration (Kresse et al. 2021). To address this, we assume two extreme cases: one where a BH is formed dynamically on short timescales of  $O(1)$  s, and another where the moderate fallback causes the mass of the protoneutron star (PNS) to exceed the maximum mass, resulting in the formation of a BH at later stages on timescales of  $> O(10)$  s. Since the former case is similar to that of the failed SNe, we adopt the same spectral model of the emitted neutrinos as the failed SNe for the prompt BH-formation case. On the other hand, as for the case of fallback induced BH formation, we construct a neutrino spectrum in the present paper. In the following, we describe the model of emitted neutrinos from fallback induced BH formation.

We combine the model of stellar core collapse in Nakazato et al. (2021) and the model of fallback mass accretion in Akaho et al. (2024) for the evaluation of the neutrino spectrum from the fallback induced BH formation. In Akaho et al. (2024), the neutrino luminosity emitted by fallback mass accretion onto a PNS with the gravitational mass of  $1.98M_\odot$ , whose baryon mass corresponds to  $2.35M_\odot$ , is provided.

So as to estimate the neutrino spectrum emitted during the early dynamical phase, we utilize the core-collapse simulation of a  $30M_\odot$  progenitor in Nakazato et al. (2021). We integrate the neutrino emission of this model up to the point where a baryon mass of the PNS reaches  $2.35M_\odot$ . While three models with differ-

ent nuclear equation of state (EOS) are presented in Nakazato et al. (2021), we adopt the model with the Togashi EOS (Togashi et al. 2017) in this study. Note that, the Furusawa-Togashi EOS (Furusawa et al. 2017) is used in the fallback model of Akaho et al. (2024) and it is different from the Togashi EOS in the low density regime. Nevertheless, the impact of their difference is minor on the neutrino emission during the early dynamical phase (Sumiyoshi et al. 2023).

In the fallback mass accretion model of Akaho et al. (2024), the inside PNS is assumed to have an isotropic temperature of  $T = 2$  MeV. In contrast, the temperature of the PNS is  $T \sim O(10)$  MeV when the baryon mass reaches  $2.35M_\odot$  in Nakazato et al. (2021). Therefore, in order to bridge the temperature gap, we perform the cooling simulation of the PNS and assess the neutrino emission. For this purpose, we adopt the structure of PNS obtained by the core-collapse simulation in Nakazato et al. (2021) as the initial condition. As for the EOS, Furusawa-Togashi EOS is adopted. Our numerical methods for the PNS cooling are similar to those employed in Suzuki (1994) and Nakazato et al. (2013). As a result of the simulation, we find that the PNS cools to  $T \sim 2$  MeV over a period of 200 s. Since the effect of convection is not taken into account in this evaluation, the cooling time might be shorter. Nevertheless, since the total energy of neutrinos emitted from the PNS cooling stems from the binding energy of PNS, the time-integrated spectrum is insensitive to the cooling time.

We also incorporate the neutrinos emitted from the fallback mass accretion based on Akaho et al. (2024). Here, we consider the fallback mass accretion of  $0.002M_\odot \text{ s}^{-1}$  onto a PNS with the gravitational mass of  $1.98M_\odot$ . Since, based on their adopted EOS, the maximum baryon mass of the NSs is  $2.70M_\odot$  and baryon mass of our PNS is  $2.35M_\odot$ , it takes 175 s to form a BH by the accretion of  $0.35M_\odot$ . Thus, the total amount of neutrinos emitted from the fallback mass accretion would be evaluated by integrating the emission rate of this model over 175 s. However, it is noted that, since the neutrino luminosity shown in Akaho et al. (2024) includes the emission from the PNS in quasi-steady state, we should subtract its contribution to avoid duplication with the contribution of PNS cooling evaluated above. As shown in Fig. 7 of Akaho et al. (2024), the neutrino luminosity and the mass accretion rate exhibit a linear relationship with an offset. This offset can be evaluated by extrapolation and regarded as the emission from the PNS. Therefore, we subtract the offset spectrum to incorporate the net contribution of the fallback mass ac-

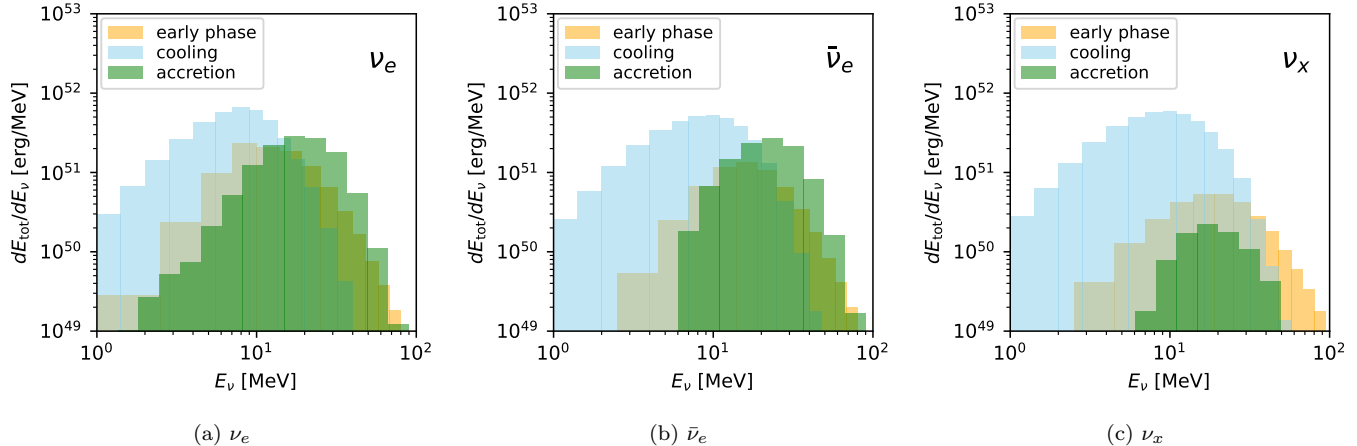


**Figure 1.** Time integrated spectra of (a)  $\nu_e$ , (b)  $\bar{\nu}_e$ , and (c)  $\nu_x$ , where  $\nu_x = \nu_\mu = \bar{\nu}_\mu = \nu_\tau = \bar{\nu}_\tau$ , for the fallback induced BH formation model. Orange, blue, and green histograms correspond to the components of the early dynamical phase, the PNS cooling, and the fallback mass accretion, respectively.

**Table 1.** Properties of emitted neutrinos for the models considered in this study.

Model	explosion		$\langle E_{\nu_e} \rangle$	$\langle E_{\bar{\nu}_e} \rangle$	$\langle E_{\nu_x} \rangle$	$E_{\nu_e, \text{tot}}$	$E_{\bar{\nu}_e, \text{tot}}$	$E_{\nu_x, \text{tot}}$
	remnant		(MeV)			$(10^{52} \text{ erg})$		
Ordinary core-collapse SN	successful	NS	9.2	10.9	11.8	4.47	4.07	4.37
BH-forming SN, (i) fallback induced	successful	BH	11.8	13.6	10.9	19.48	18.50	12.07
BH-forming SN, (ii) prompt	successful	BH	16.1	20.4	23.4	6.85	5.33	2.89
Failed SN	failed	BH	16.1	20.4	23.4	6.85	5.33	2.89

NOTE— $\langle E_{\nu_i} \rangle$  and  $E_{\nu_i, \text{tot}}$  are the average and total energies of the time-integrated neutrino signal for  $\nu_i$ , where  $\nu_x$  represents the average of  $\nu_\mu$ ,  $\bar{\nu}_\mu$ ,  $\nu_\tau$ , and  $\bar{\nu}_\tau$ .

cretion. Owing to the subtraction, the total amount of neutrinos emitted from the fallback mass accretion is insensitive to the choice of mass accretion rate, provided that the accreted mass is fixed to  $0.35M_\odot$ .

In Fig. 1, we show the neutrino spectra of individual components: the early dynamical phase, the PNS cooling, and the fallback mass accretion. A substantial amount of  $\nu_e$  and  $\bar{\nu}_e$  are emitted from the fallback mass accretion. These neutrinos have high average energies and they are mainly produced by electron capture and positron capture. Fallback mass accretion produces the high-temperature environment where thermal electrons and positrons are created and supplies enormous free protons and neutrons which capture electrons and positrons, respectively. In contrast, the amount of  $\nu_x$  ( $= \nu_\mu = \bar{\nu}_\mu = \nu_\tau = \bar{\nu}_\tau$ ) emitted from the fallback mass accretion is much smaller than those of  $\nu_e$  and  $\bar{\nu}_e$ . According to Akaho et al. (2024), the primary process for emitting  $\nu_x$  is nucleon-nucleon bremsstrahlung, which is

efficient in the high density regions inside the PNS, and the luminosity of  $\nu_x$  is hardly dependent on the accretion rate. Therefore, due to the subtraction considered in this study, the contribution of fallback mass accretion is minor for  $\nu_x$ .

In Table 1, the average and total energies of neutrinos emitted from the fallback induced BH-forming SN are compared with other scenarios taken into account in this study. The total emission energy of neutrinos, summing all flavors, amounts to  $8.63 \times 10^{53}$  erg. Since the binding energy of the maximum-mass NS is  $8.78 \times 10^{53}$  erg for the EOS adopted here, our fallback induced BH formation can be interpreted as maximizing the emission energy of neutrinos from a single stellar collapse<sup>1</sup>. On the other hand, as already mentioned, we assume that the neu-

<sup>1</sup> Except for the collapse of supermassive stars with  $\gtrsim 10^3 M_\odot$  (e.g., Nakazato et al. 2006).

trino signal of the prompt BH-forming SN is same as the failed SN (BH formation without explosion). The total emission energy of neutrinos, summing all flavors, is  $2.37 \times 10^{53}$  erg, which is 28% of the fallback induced BH formation model. Then, we consider that the uncertainty in the neutrino emission from BH-forming SNe is accounted for both extremes.

### 3. DSNB FLUX MODEL

Following [Ashida et al. \(2023\)](#), we describe the DSNB flux as

$$\frac{d\Phi(E_\nu)}{dE_\nu} = c \int_0^{z_{\max}} \frac{dz}{H_0 \sqrt{\Omega_m(1+z)^3 + \Omega_\Lambda}} \times \left[ R_{\text{SN}}(z) \left\{ (1 - f_{\text{BHNS}}) \frac{dN_{\text{CCSN}}(E'_\nu)}{dE'_\nu} + f_{\text{BHNS}} \frac{dN_{\text{BHNS}}(E'_\nu)}{dE'_\nu} \right\} + R_{\text{BH}}(z) \frac{dN_{\text{BH}}(E'_\nu)}{dE'_\nu} \right], \quad (1)$$

where  $c$  is the speed of light and the cosmological constants are  $\Omega_m = 0.3089$ ,  $\Omega_\Lambda = 0.6911$ , and  $H_0 = 67.74 \text{ km sec}^{-1} \text{ Mpc}^{-1}$ . The neutrino energy at a detector,  $E_\nu$ , and a source,  $E'_\nu$ , are related to the redshift of the source,  $z$ , as  $E'_\nu = (1+z)E_\nu$ , where the range of redshift is set to  $0 \leq z \leq z_{\max} = 5$ . As for the neutrino sources, we consider ordinary core-collapse SNe, BH-forming SNe, and failed SNe, whose spectra are denoted as,  $dN_{\text{CCSN}}(E'_\nu)/dE'_\nu$ ,  $dN_{\text{BHNS}}(E'_\nu)/dE'_\nu$ , and  $dN_{\text{BH}}(E'_\nu)/dE'_\nu$  respectively. For  $dN_{\text{CCSN}}(E'_\nu)/dE'_\nu$  and  $dN_{\text{BH}}(E'_\nu)/dE'_\nu$ , we adopt the same models as [Ashida et al. \(2023\)](#), but we only investigate the case of Toghiani EOS. The model of an ordinary core-collapse SN corresponds to the case where a  $1.32M_\odot$  NS is formed from the collapse of a  $15M_\odot$  progenitor, while the model of a failed SN corresponds to the case where a BH is formed without an explosion from the collapse of a  $30M_\odot$  progenitor ([Ashida & Nakazato 2022](#)). As stated in § 2, we investigate two cases: (i) fallback induced and (ii) prompt BH-forming SNe (Table 1) for  $dN_{\text{BHNS}}(E'_\nu)/dE'_\nu$ .

In eq. (1),  $R_{\text{SN}}(z)$  and  $R_{\text{BH}}(z)$  are rates of successful SNe and failed SNe, respectively, as functions of redshift. We adopt  $R_{\text{SN}}(z)$  and  $R_{\text{BH}}(z)$  deduced from the model of galactic chemical evolution in [Tsujiimoto \(2023\)](#), which are also investigated in [Ashida et al. \(2023\)](#) as a reference model (see Table 1 of that paper). This model exhibits two distinct features. Firstly, the stellar IMF depends on the type of galaxies (e.g., [Hopkins 2018](#)); the early-type galaxies, which are formed in bursty star formation, have a flat IMF (a slope index of a power law  $x = -0.9$ ) and efficiently eject heavy elements while the late-type galaxies have the Salpeter IMF ( $x = -1.35$ ). Secondly, the upper bound on the mass

of core-collapse SN progenitors is  $18M_\odot$  (e.g., [Smartt 2009, 2015](#); [Sukhbold et al. 2016](#); [Kresse et al. 2021](#)); a mass range of progenitors is  $8\text{--}18M_\odot$  for core-collapse SNe and  $18\text{--}100M_\odot$  for failed SNe. The predicted redshift evolution of  $R_{\text{SN}}$  is in better agreement with the measured rates. On the other hand,  $R_{\text{BH}}$  corresponds to the rate of BH formations without SN explosions. In the present study, core-collapse SNe are classified into two categories: ordinary core-collapse SNe, which leave NSs, and BH-forming SNe. For simplicity, we assume that the fraction of BH-forming SNe, denoted as  $f_{\text{BHNS}}$ , does not depend on the redshift.

In [Tsujiimoto \(2023\)](#),  $R_{\text{SN}}(z)$  and  $R_{\text{BH}}(z)$  are calculated by converting from observationally estimated cosmic star formation rate (SFR). For this purpose, SFRs of [Madau & Dickinson \(2014\)](#) and [Hopkins & Beacom \(2006\)](#), which are referred to as MD14 and HB06, respectively, are used. We also investigate the both cases in this paper.

Since neutrinos undergo flavor oscillations before the detection, we take into account the so-called MSW effect ([Wolfenstein 1978](#); [Mikheyev & Smirnov 1985](#)) following [Nakazato et al. \(2015\)](#). The survival probability of  $\bar{\nu}_e$ ,  $\bar{P}$ , depends on the neutrino mass hierarchy ([Dighe & Smirnov 2000](#)) as  $\bar{P} = \cos^2 \theta_{12} \cos^2 \theta_{13}$  for the normal mass hierarchy (NH) and  $\bar{P} = \sin^2 \theta_{13}$  for the inverted mass hierarchy (IH), where  $\theta_{12}$  and  $\theta_{13}$  are mixing angles. Since recent measurements for them are  $\sin^2 \theta_{12} \approx 0.31$  and  $\sin^2 \theta_{13} \approx 0.02$  ([Workman et al. 2022](#)), we set  $\bar{P} = 0.68$  for NH and  $\bar{P} = 0.02$  for IH in this study.

In Fig. 2, the  $\bar{\nu}_e$  flux estimated by the DSNB model described above is compared with the latest experimental upper bounds. The largest flux is provided by the model with NH, HB06 SFR, and fallback induced BH formation for the following reason. In the case of fallback induced BH formation, the binding energy of the maximum-mass NS is converted to the total emission energy of neutrinos. Since, as already stated, the fallback mass accretion emits a much larger amount of  $\bar{\nu}_e$  than  $\nu_x$ , the terrestrial DSNB flux is larger for NH, which has higher survival probability of  $\bar{\nu}_e$  than IH. If the fraction of BH-forming SNe is  $f_{\text{BHNS}} = 0.5$  for NH, the DSNB flux exceeds the upper bounds in several energy bins. As shown in Fig. 3, where the integrated fluxes with  $E_\nu > 17.3 \text{ MeV}$  are compared with the 90% C.L. upper limits and best-fit results in [Abe et al. \(2021b\)](#), the models of fallback induced BH formation has a constraint of  $f_{\text{BHNS}} < 0.45$  (0.26) for the case with NH and MD14 (HB06) SFR.

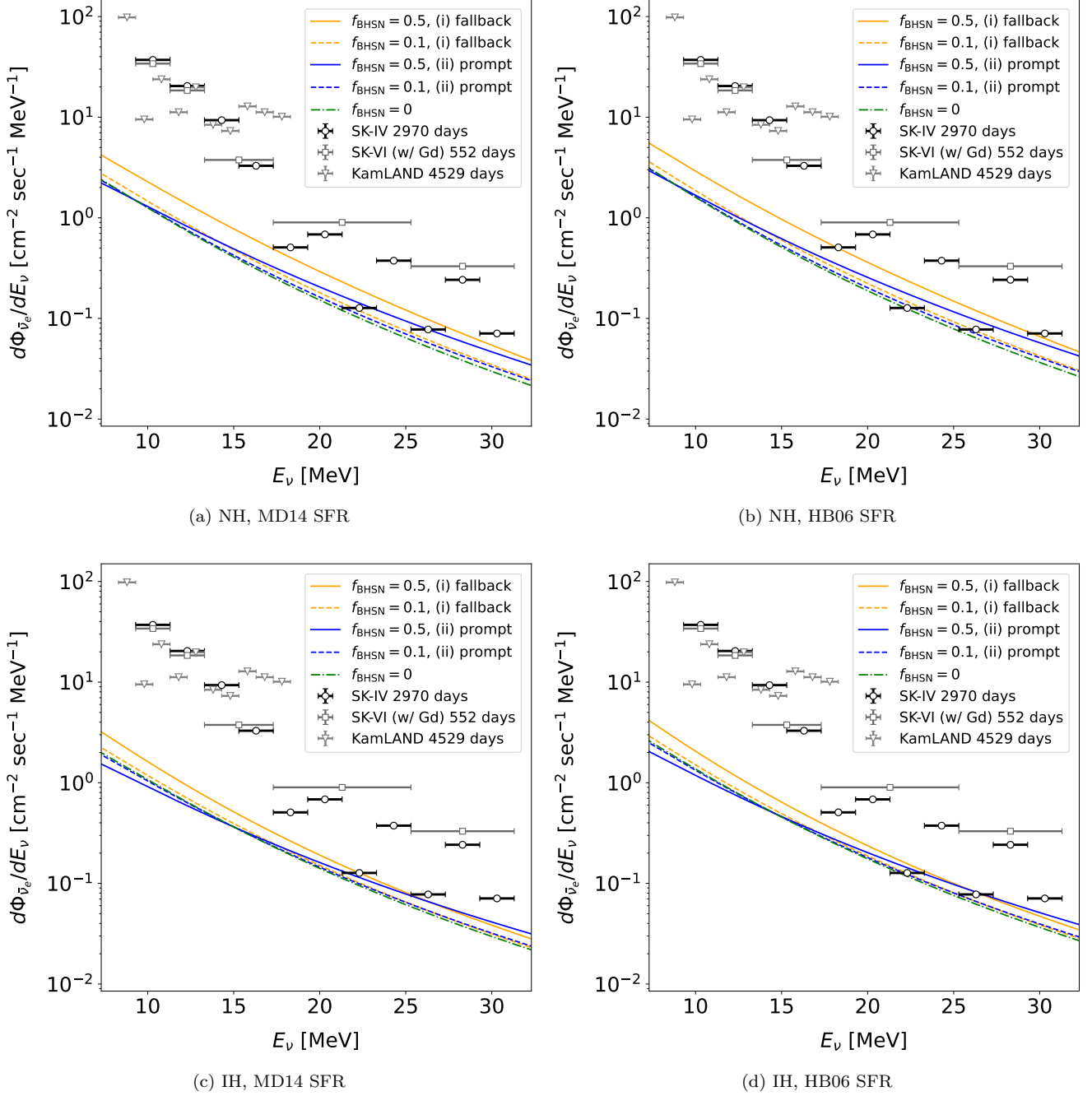
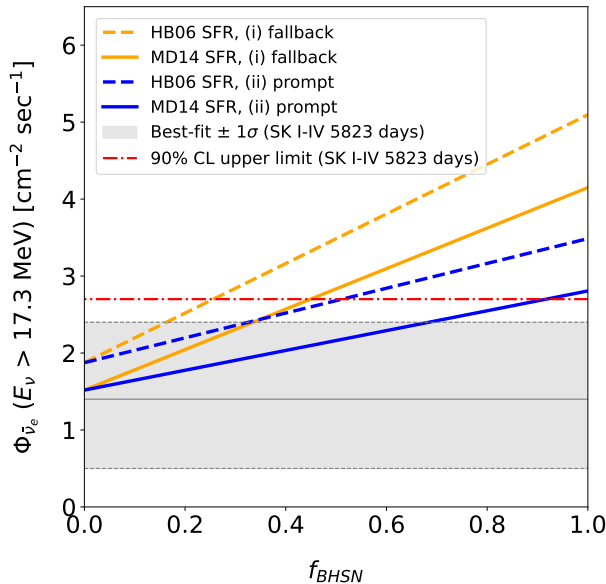
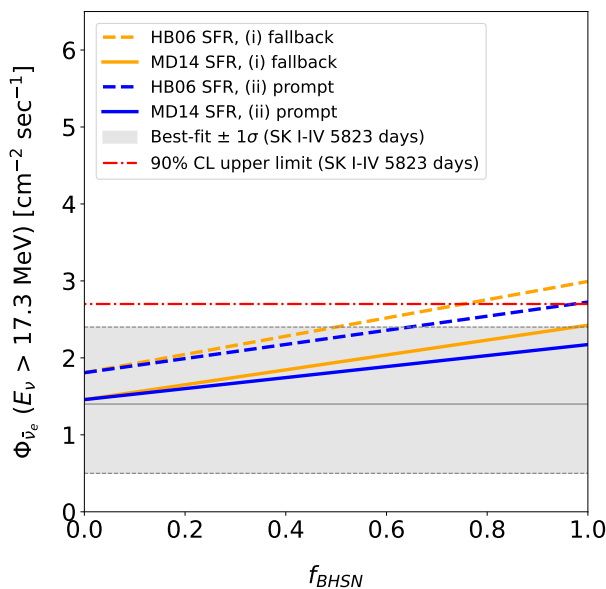


**Figure 2.** Spectra of cosmic background  $\bar{\nu}_e$  flux from this study compared with the 90% confidence level upper bounds from SK with pure (Abe et al. 2021b) and gadolinium-loaded (Harada et al. 2023b) water, and KamLAND (Abe et al. 2022). Models with different mass hierarchy and SFR are shown in each panel: (a) NH and MD14, (b) NH and HB06, (c) IH and MD14, and (d) IH and HB06. Solid, dashed, and dot-dashed lines show the spectra estimated with  $f_{\text{BHSN}} = 0.5, 0.1,$  and  $0,$  respectively, where  $f_{\text{BHSN}}$  is the fraction of successful SN explosions that form a BH. Orange and blue lines correspond to (i) fallback induced and (ii) prompt BH-formation cases, respectively, in Table 1.



(a) NH



(b) IH

**Figure 3.** The integrated  $\bar{\nu}_e$  flux with  $E_\nu > 17.3$  MeV estimated by our DSNB models in comparison with the best-fit values and their  $\pm 1\sigma$  uncertainties shown in grey solid lines and shaded regions, respectively, and the 90% observed upper limits shown in red dot-dashed lines from SK with pure water (Abe et al. 2021b). Note that these experimental constraints are associated with the spectral models in Nakazato et al. (2015) while they are insensitive to the adopted spectrum models. Models with different mass hierarchy are shown in each panel: (a) NH and (b) IH. Solid and dashed lines represent the spectra for the models with MD14 SFR and HB06 SFR, respectively. Orange and blue lines correspond to (i) fallback induced and (ii) prompt BH-formation cases, respectively, in Table 1.

#### 4. EVENT RATE AND EXPERIMENTAL SENSITIVITY

In this section, we investigate the event rate spectra and the experimental sensitivity to our DSNB models following Ashida & Nakazato (2022). Water Cherenkov detectors, such as SK and HK, detect the DSNB via inverse beta decay (IBD) of  $\bar{\nu}_e$ :

$$\bar{\nu}_e + p \rightarrow e^+ + n. \quad (2)$$

Thus, the DSNB event rate is calculated as

$$\frac{dN_{\text{event}}(E_{e^+})}{dE_{e^+}} = N_p \cdot \sigma_{\text{IBD}}(E_\nu) \cdot \frac{d\Phi_{\bar{\nu}_e}^{\text{det}}(E_\nu)}{dE_\nu}, \quad (3)$$

where  $\sigma_{\text{IBD}}(E_\nu)$  is the IBD cross section taken from Strumia & Vissani (2003) and  $d\Phi_{\bar{\nu}_e}^{\text{det}}(E_\nu)/dE_\nu$  is terrestrial flux of  $\bar{\nu}_e$ . The positron energy  $E_{e^+}$  is related to the neutrino energy  $E_\nu$  as  $E_{e^+} = E_\nu - \Delta c^2$ , where  $\Delta$  is a neutron-proton mass difference, and  $N_p$  represents the number of free protons contained in the fiducial volume of the detector, which is  $N_p = 1.5 \times 10^{33}$  for SK and  $N_p = 12.6 \times 10^{33}$  for HK.

The event rate spectra at SK from our DSNB models with MD14 SFR are shown in Fig. 4. Incidentally, HK has a  $\sim 8.4$  times higher event rate than SK and the model with HB06 SFR has a  $\sim 1.24$  times higher event rate than that with MD14 SFR. If there are no BH-forming SNe ( $f_{\text{BH-SN}} = 0$ ), the expected number of IBD signal events with  $17.3 < E_\nu < 31.3$  MeV is 180 (170) for the model with NH (IH) and MD14 SFR at HK over 10 yr.<sup>2</sup> If the contributions of fallback induced BH-forming SNe are included and  $f_{\text{BH-SN}} = 0.5$  is assumed, the event number increases to 340 for NH and 230 for IH. On the other hand, in the case of prompt BH-forming SNe and  $f_{\text{BH-SN}} = 0.5$ , the event number is 260 for NH and 210 for IH. The impact on the event number is largest for the case with NH and fallback induced BH-forming SNe. However, for the other cases also, the event numbers increase due to the BH-forming SNe while the impacts are not so large. This is because high-energy neutrino emission in the early dynamical phase is more efficient compared to ordinary core-collapse SNe. In any case, the inclusion of BH-forming SNe favors the detection of DSNB. Incidentally, it reduces the number of IBD signal events with  $E_\nu < 13.3$  MeV, where many background events exist at HK, for the case with IH and prompt BH-forming SNe. This is because low-energy neutrinos are mainly emitted from the cooling of the PNS, which is not included in the prompt BH formation case.

<sup>2</sup> The event number is reduced to 50–60 when the detection efficiency including neutron tag is taken into account (Ashida et al. 2023).

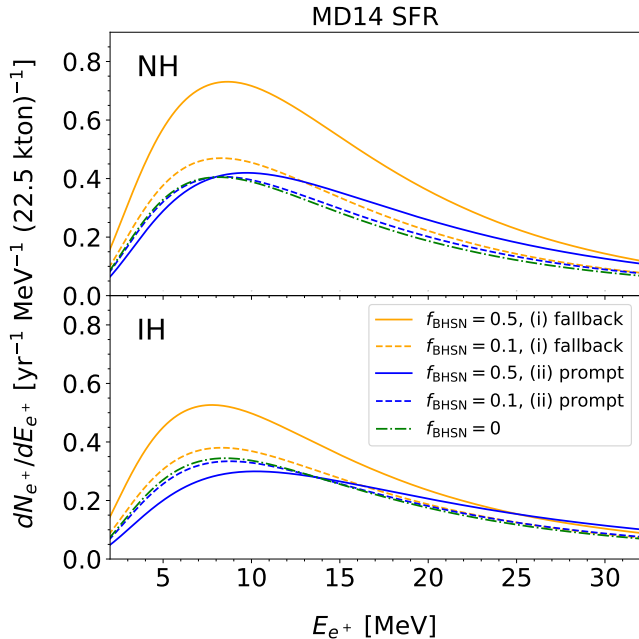


**Figure 4.** Predicted DSNB event rate spectra at SK (a water volume of 22.5 kton) per year with different choices of the BH-forming SNe model and  $f_{\text{BHSN}}$  for NH (top) and IH (bottom) and MD14 SFR. The notation of lines is the same as in Fig. 2.

Now we move on to the experimental sensitivity. The expected upper bound on the integrated flux of  $\bar{\nu}_e$  with  $17.3 < E_\nu < 31.3$  MeV is calculated as (Abe et al. 2021b; Ashida & Nakazato 2022)

$$\Phi_{\text{lim}} = \frac{N_{\text{lim}}}{T \cdot N_p \cdot \bar{\sigma}_{\text{IBD}} \cdot \epsilon_{\text{sig}}}, \quad (4)$$

where  $N_{\text{lim}}$  is the upper bound on the number of events for the given operation time  $T$ . The IBD cross section at  $E_\nu = 24.3$  MeV is used for the averaged cross section  $\bar{\sigma}_{\text{IBD}}$ . In the following, we consider the sensitivity at HK. The signal efficiency assumed in this study ( $\epsilon_{\text{sig}}$ ) is taken from the former SK analysis (Abe et al. 2021b), as was done in our previous study (Ashida & Nakazato 2022), which is around 20% to 30% depending on energy. As is done at SK, we assume that the IBD reaction of  $\bar{\nu}_e$  is identified by the coincidence of the Cherenkov light emitted from the positron and the 2.2 MeV  $\gamma$  ray emitted from neutron capture on hydrogen. This method is called neutron tagging and the signal efficiency becomes not very high due to the low energy of this  $\gamma$  ray.

For a certain confidence level (C.L.),  $N_{\text{lim}}$  is obtained as the excess of the observation over the background expectation, where the statistical and systematic uncertainties of the background events are taken into account. The background at HK in higher energies ( $E_\nu > 17.3$  MeV) mainly stems from atmospheric

neutrinos and is classified into two categories: neutral-current quasielastic (NCQE) interactions and others (non-NCQE). In the NCQE interactions, a neutrino often knocks a neutron out of an oxygen nucleus, where the  $\gamma$  ray emitted from the deexcitation of the residual nucleus and the knocked out neutron mimic the positron signal from IBD. The size of the NCQE background assumed in the present study is scaled from that at the past SK experiment (Abe et al. 2021b). The systematic uncertainty of the NCQE background is assumed to decrease year by year (see Table 1 of Ashida & Nakazato 2022) due to expected efforts in accelerator neutrino and nuclear experiments (Abe et al. 2019; Ashida et al. 2024; Tano et al. 2024). As for the non-NCQE background, we consider the following interactions: charged-current interaction of atmospheric  $\bar{\nu}_e$ , which produces a positron and a neutron as in IBD, charged-current muon neutrino interaction, and some of neutral-current interactions involving a low-energy pion. In the latter two interactions, a visible positron from the decay of an invisible muon becomes background in the DSNB search because a neutron produced by the parent reaction may be tagged or, even without a neutron, an accidental coincidence with noise might occur. The size and systematic uncertainty of the non-NCQE backgrounds are again extrapolated from the SK experiment in this study. In addition, we also take into account the background due to spallation of oxygen nuclei induced by energetic atmospheric muons, which produces radioactive isotopes and leads to misidentification as IBD events. HK is expected to suffer from the four times higher spallation background event rate per volume compared to SK due to the shallower depth of its construction site (Abe et al. 2018). Not only the isotopes with  $\beta+n$  decay, such as  ${}^9\text{Li}$ , increase, but also the likelihood of accidental coincidences becomes higher. We then increase both  ${}^9\text{Li}$  and accidental backgrounds by a factor of four compared to the ones in Ashida & Nakazato (2022)<sup>3</sup>.

Using  $\Phi_{\text{lim}}$  obtained by eq. (4), we evaluate the operation time required to detect the DSNB at HK for our models. This is shown in Fig. 5 as a function of  $f_{\text{BHSN}}$  for different cases and C.L. We found that the DSNB detection would be achieved within at most  $\sim 6$  yr at  $2\sigma$  and  $\sim 20$  yr at  $3\sigma$ , and including the BH-forming SNe reduces the required operation time in any case. Furthermore, the impact of BH-forming SNe is significant in some cases; the operation time required for  $3\sigma$  is short-

<sup>3</sup> This is rather a conservative estimation because the accidental background in the energy range of the present analysis is not necessarily made by spallation but partially by atmospheric events as well.



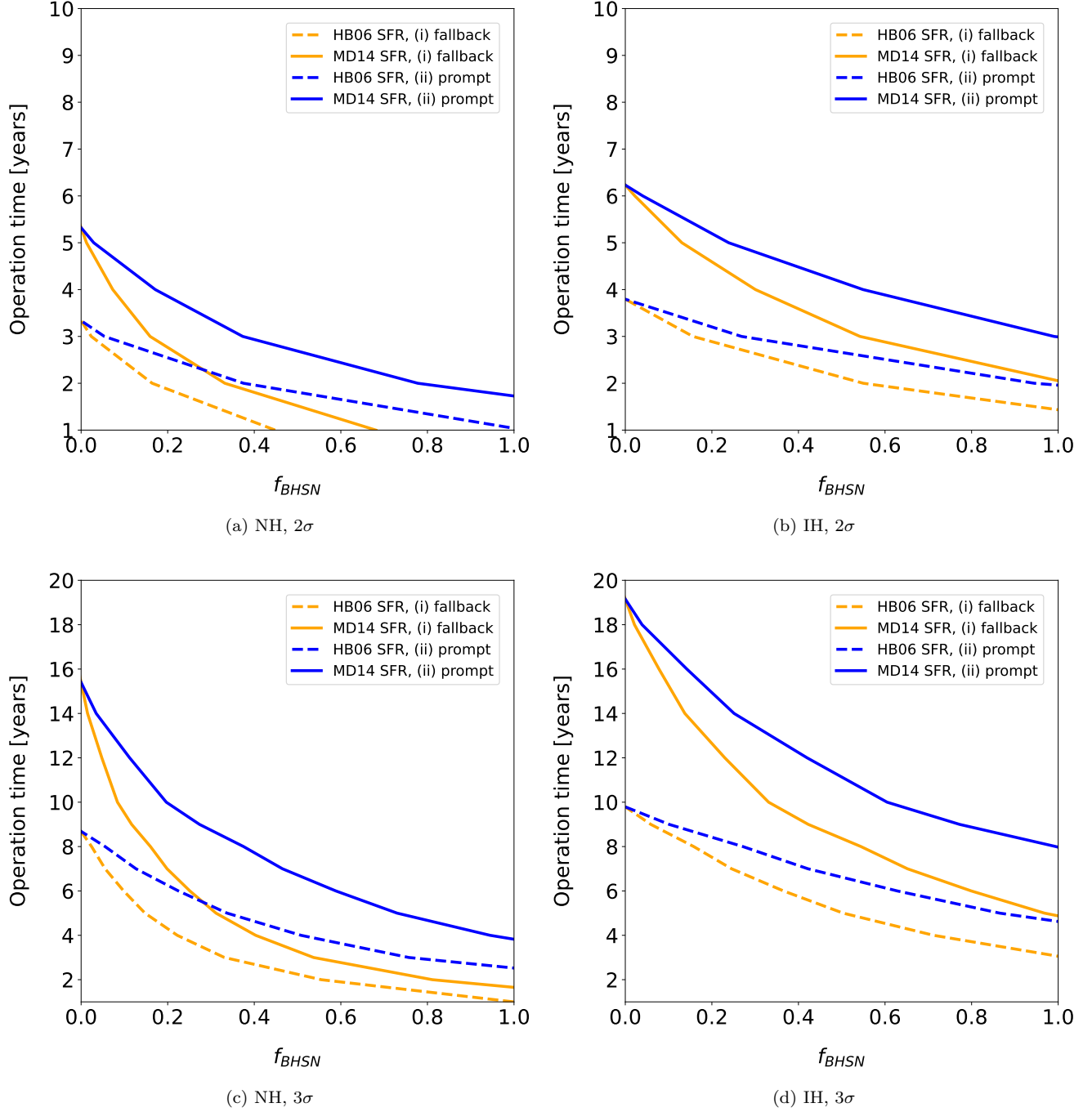


**Figure 5.** Operation time required to detect the DSNB at HK as a function of the fraction of BH-forming SNe,  $f_{BHSN}$ , based on our models with different mass hierarchy at different C.L.: (a) NH and  $2\sigma$ , (b) IH and  $2\sigma$ , (c) NH and  $3\sigma$ , and (d) IH and  $3\sigma$ . The notation of lines is the same as in Fig. 3.

ened by half with  $f_{\text{BH-SN}} = 0.2$  for the model of fallback induced BH formation, NH, and MD14 SFR. Otherwise, the upper bound on  $f_{\text{BH-SN}}$  would be provided within the expected operational period of HK.

## 5. SUMMARY AND DISCUSSION

In this study, we have constructed a new DSNB model that includes the contribution of BH-forming SNe, which lead to both a successful SN explosion and BH formation simultaneously. According to studies on Galactic chemical evolution and nucleosynthesis, the population of BH-forming SNe is implied to be non-negligible in accounting for the observed abundance of some heavy elements. Since the detailed dynamics and neutrino emission of BH-forming SNe are uncertain, we have considered two extreme cases: fallback-induced BH formation and prompt BH formation. In the first scenario, a longer duration until BH formation ensures significant neutrino emission, and the total energy of emitted neutrinos in our model is consistent with the binding energy of a maximum-mass NS. On the other hand, in the second scenario, the shorter duration results in reduced neutrino emission. The rates of successful SNe (the sum of ordinary core-collapse SNe and BH-forming SNe) and failed SNe (BH formation without SN explosions) have been based on the model of galactic chemical evolution in [Tsujiimoto \(2023\)](#). As a result, we have found that the contribution of BH-forming SNe enhances the flux and event rate of the DSNB at high energies ( $E_\nu > 17.3$  MeV). In particular, the impacts are largest in the case of fallback-induced BH formation with neutrino oscillation in NH since the fallback mass accretion onto a PNS emits a much larger amount of  $\bar{\nu}_e$  than  $\nu_x$ . In this case, the expected event rate at  $E_\nu > 17.3$  MeV doubles if the fraction of BH-forming SNe is  $f_{\text{BH-SN}} = 0.5$ . Furthermore, with  $f_{\text{BH-SN}} = 0.2$ , the operation time required for  $3\sigma$  detection at HK is shortened by half, assuming MD14 SFR. Similarly, in other cases, the required operation time is also reduced due to the contribution of BH-forming SNe.

Concerning the treatment of BH-forming SNe, there is room for further improvement. In this paper, we have avoided specifying the dynamics of BH-forming SNe and instead focused on discussing two extreme cases of neutrino emission. In actual conditions, the amount of neutrino emission may lie between these two extremes or vary widely. While numerical examples are still limited, the model of [Burrows et al. \(2023\)](#) has a short time to BH formation of less than 2 s, which can be considered to be similar to our prompt BH formation model. Incidentally, [Kresse et al. \(2021\)](#) shows that even failed SNe may take around 10 s to form a BH. The time to BH for-

mation is heavily dependent on the efficiency of fallback mass accretion, which is significantly determined by the structure of the progenitor. Therefore, it is worthwhile to investigate the neutrino emissions from BH-forming SNe using the same progenitor models employed in studies of nucleosynthesis and chemical evolution.

In the present study, we assume that BH-forming SNe reside within the mass range of  $8\text{--}18M_\odot$  according to the observed implication ([Smartt 2009, 2015](#)). In contrast, the arguments based on nucleosynthesis/chemical evolution have been done under the hypothesis that the progenitor masses of BH-forming SNe would be larger than  $20M_\odot$  (e.g., [Kobayashi et al. 2006](#); [Pignatari et al. 2023](#)). Thus, there is a clear inconsistency between the two. While our results depend mainly on the fraction of BH-forming SNe, i.e.,  $f_{\text{BH-SN}}$ , for the given rate of successful SNe, i.e.,  $R_{\text{SN}}$ , regardless of their progenitor masses, it is worthwhile to discuss how the observed upper mass bound ( $18M_\odot$ ) can be reconciled with their masses ( $> 20M_\odot$ ) implied from the theoretical argument based on nucleosynthesis.

One possible explanation is the observational bias. Many BH-forming SNe may be unnoticed if they exhibit systematically lower peak luminosities than ordinary core-collapse SNe. This possibility is quite plausible for the case of faint SNe ([Nomoto et al. 2006](#)). Even for hypernovae, such a non-detection is possible owing to their jet-like explosions; in most cases, the jets do not direct to us and the corresponding SNe seem to exhibit low brightness. Another possible solution is the metallicity-dependent frequency of BH-forming SNe; they exclusively emerge in a low-metallicity environment, which is provided by the limited regions in the local Universe. This possibility is in particular expected for hypernovae, because their progenitors are considered to be fast-rotating massive stars (e.g., [Iwamoto et al. 1998](#)) and a low metallicity helps to retain enough angular momentum (e.g., [Woosley & Heger 2006](#)). In addition, hypernovae could be closely connected to long gamma ray bursts ([Galama et al. 1998](#)), whose emergence is indeed biased toward low-metallicity ( $Z \lesssim 0.3\text{--}0.5Z_\odot$ ) galaxies ([Fruchter et al. 2006](#); [Vergani et al. 2015](#)). These arguments propose that the redshift evolution of metallicity for individual galaxies could be one of the key factors including the IMF for counting the DSNB flux, as done by [Nakazato et al. \(2015\)](#).

This work is supported by Grants-in-Aid for Scientific Research (JP18H01258, JP20K03973, JP23H00132, JP24K07021), Grant-in-Aid for Scientific Research on Innovative Areas (JP19H05811), and Grant-in-Aid for Transformative Research Areas (JP24H02245) from the Ministry of Education, Culture, Sports, Science and Technology (MEXT), Japan, and by NSF Grant No. PHY-2309967.

## REFERENCES

- Abbasi, R., Abdou, Y., Abu-Zayyad, T., et al. 2011, *A&A*, 535, A109, doi: [10.1051/0004-6361/201117810](https://doi.org/10.1051/0004-6361/201117810)
- Abe, K., Haga, Y., Hayato, Y., et al. 2016, *Astroparticle Physics*, 81, 39, doi: [10.1016/j.astropartphys.2016.04.003](https://doi.org/10.1016/j.astropartphys.2016.04.003)
- Abe, K., Abe, K., Aihara, H., et al. 2018, arXiv e-prints, arXiv:1805.04163, doi: [10.48550/arXiv.1805.04163](https://doi.org/10.48550/arXiv.1805.04163)
- Abe, K., Akutsu, R., Ali, A., et al. 2019, *PhRvD*, 100, 112009, doi: [10.1103/PhysRevD.100.112009](https://doi.org/10.1103/PhysRevD.100.112009)
- Abe, K., Adrich, P., Aihara, H., et al. 2021a, *ApJ*, 916, 15, doi: [10.3847/1538-4357/abf7c4](https://doi.org/10.3847/1538-4357/abf7c4)
- Abe, K., Bronner, C., Hayato, Y., et al. 2021b, *PhRvD*, 104, 122002, doi: [10.1103/PhysRevD.104.122002](https://doi.org/10.1103/PhysRevD.104.122002)
- Abe, S., Asami, S., Gando, A., et al. 2022, *ApJ*, 925, 14, doi: [10.3847/1538-4357/ac32c1](https://doi.org/10.3847/1538-4357/ac32c1)
- Akaho, R., Nagakura, H., & Foglizzo, T. 2024, *ApJ*, 960, 116, doi: [10.3847/1538-4357/ad118c](https://doi.org/10.3847/1538-4357/ad118c)
- Alekseev, E. N., Alekseeva, L. N., Volchenko, V. I., & Krivosheina, I. V. 1987, *Soviet Journal of Experimental and Theoretical Physics Letters*, 45, 589
- Anandagoda, S., Hartmann, D. H., Fryer, C. L., et al. 2023, *ApJ*, 950, 29, doi: [10.3847/1538-4357/acc84f](https://doi.org/10.3847/1538-4357/acc84f)
- Ando, S. 2003, *Physics Letters B*, 570, 11, doi: [10.1016/j.physletb.2003.07.009](https://doi.org/10.1016/j.physletb.2003.07.009)
- Ando, S., Ekanger, N., Horiuchi, S., & Koshio, Y. 2023, *Proceedings of the Japan Academy, Series B*, 99, 460, doi: [10.2183/pjab.99.026](https://doi.org/10.2183/pjab.99.026)
- Ando, S., & Sato, K. 2004, *New Journal of Physics*, 6, 170, doi: [10.1088/1367-2630/6/1/170](https://doi.org/10.1088/1367-2630/6/1/170)
- Ando, S., Sato, K., & Totani, T. 2003, *Astroparticle Physics*, 18, 307, doi: [10.1016/S0927-6505\(02\)00152-4](https://doi.org/10.1016/S0927-6505(02)00152-4)
- Aoyama, S., Ouchi, M., & Harikane, Y. 2023, *ApJ*, 946, 69, doi: [10.3847/1538-4357/acba87](https://doi.org/10.3847/1538-4357/acba87)
- Ashida, Y. 2024, arXiv e-prints, arXiv:2401.12403, doi: [10.48550/arXiv.2401.12403](https://doi.org/10.48550/arXiv.2401.12403)
- Ashida, Y., & Nakazato, K. 2022, *ApJ*, 937, 30, doi: [10.3847/1538-4357/ac8a46](https://doi.org/10.3847/1538-4357/ac8a46)
- Ashida, Y., Nakazato, K., & Tsujimoto, T. 2023, *ApJ*, 953, 151, doi: [10.3847/1538-4357/ace3ba](https://doi.org/10.3847/1538-4357/ace3ba)
- Ashida, Y., Nagata, H., Mori, M., et al. 2024, *PhRvC*, 109, 014620, doi: [10.1103/PhysRevC.109.014620](https://doi.org/10.1103/PhysRevC.109.014620)
- Bays, K., Iida, T., Abe, K., et al. 2012, *PhRvD*, 85, 052007, doi: [10.1103/PhysRevD.85.052007](https://doi.org/10.1103/PhysRevD.85.052007)
- Beacom, J. F. 2010, *Annual Review of Nuclear and Particle Science*, 60, 439, doi: [10.1146/annurev.nucl.010909.083331](https://doi.org/10.1146/annurev.nucl.010909.083331)
- Beacom, J. F., & Vagins, M. R. 2004, *PhRvL*, 93, 171101, doi: [10.1103/PhysRevLett.93.171101](https://doi.org/10.1103/PhysRevLett.93.171101)
- Bionta, R. M., Blewitt, G., Bratton, C. B., et al. 1987, *PhRvL*, 58, 1494, doi: [10.1103/PhysRevLett.58.1494](https://doi.org/10.1103/PhysRevLett.58.1494)
- Bisnovatyi-Kogan, G. S., & Seidov, Z. F. 1982, *Soviet Ast.*, 26, 132
- Burrows, A., Vartanyan, D., & Wang, T. 2023, *ApJ*, 957, 68, doi: [10.3847/1538-4357/acfc1c](https://doi.org/10.3847/1538-4357/acfc1c)
- Dar, A. 1985, *PhRvL*, 55, 1422, doi: [10.1103/PhysRevLett.55.1422](https://doi.org/10.1103/PhysRevLett.55.1422)
- de Gouvêa, A., Martinez-Soler, I., Perez-Gonzalez, Y. F., & Sen, M. 2020, *PhRvD*, 102, 123012, doi: [10.1103/PhysRevD.102.123012](https://doi.org/10.1103/PhysRevD.102.123012)
- . 2022, *PhRvD*, 106, 103026, doi: [10.1103/PhysRevD.106.103026](https://doi.org/10.1103/PhysRevD.106.103026)
- Dighe, A. S., & Smirnov, A. Y. 2000, *PhRvD*, 62, 033007, doi: [10.1103/PhysRevD.62.033007](https://doi.org/10.1103/PhysRevD.62.033007)
- Ekanger, N., Horiuchi, S., Kotake, K., & Sumiyoshi, K. 2022, *PhRvD*, 106, 043026, doi: [10.1103/PhysRevD.106.043026](https://doi.org/10.1103/PhysRevD.106.043026)
- Ekanger, N., Horiuchi, S., Nagakura, H., & Reitz, S. 2024, *PhRvD*, 109, 023024, doi: [10.1103/PhysRevD.109.023024](https://doi.org/10.1103/PhysRevD.109.023024)
- Fogli, G. L., Lisi, E., Mirizzi, A., & Montanino, D. 2004, *PhRvD*, 70, 013001, doi: [10.1103/PhysRevD.70.013001](https://doi.org/10.1103/PhysRevD.70.013001)
- Fruchter, A. S., Levan, A. J., Strolger, L., et al. 2006, *Nature*, 441, 463, doi: [10.1038/nature04787](https://doi.org/10.1038/nature04787)
- Fujibayashi, S., Yoshida, T., & Sekiguchi, Y. 2015, *ApJ*, 810, 115, doi: [10.1088/0004-637X/810/2/115](https://doi.org/10.1088/0004-637X/810/2/115)
- Furusawa, S., Togashi, H., Nagakura, H., et al. 2017, *Journal of Physics G Nuclear Physics*, 44, 094001, doi: [10.1088/1361-6471/aa7f35](https://doi.org/10.1088/1361-6471/aa7f35)

- Galais, S., Kneller, J., Volpe, C., & Gava, J. 2010, *PhRvD*, 81, 053002, doi: [10.1103/PhysRevD.81.053002](https://doi.org/10.1103/PhysRevD.81.053002)
- Galama, T. J., Vreeswijk, P. M., van Paradijs, J., et al. 1998, *Nature*, 395, 670, doi: [10.1038/27150](https://doi.org/10.1038/27150)
- Gando, A., Gando, Y., Ichimura, K., et al. 2012, *ApJ*, 745, 193, doi: [10.1088/0004-637X/745/2/193](https://doi.org/10.1088/0004-637X/745/2/193)
- Harada, A., Suwa, Y., Harada, M., et al. 2023a, *ApJ*, 954, 52, doi: [10.3847/1538-4357/ace52e](https://doi.org/10.3847/1538-4357/ace52e)
- Harada, M., Abe, K., Bronner, C., et al. 2023b, *ApJL*, 951, L27, doi: [10.3847/2041-8213/acdc9e](https://doi.org/10.3847/2041-8213/acdc9e)
- Hartmann, D. H., & Woosley, S. E. 1997, *Astroparticle Physics*, 7, 137, doi: [10.1016/S0927-6505\(97\)00018-2](https://doi.org/10.1016/S0927-6505(97)00018-2)
- Heger, A., Fryer, C. L., Woosley, S. E., Langer, N., & Hartmann, D. H. 2003, *ApJ*, 591, 288, doi: [10.1086/375341](https://doi.org/10.1086/375341)
- Hirata, K., Kajita, T., Koshiba, M., et al. 1987, *PhRvL*, 58, 1490, doi: [10.1103/PhysRevLett.58.1490](https://doi.org/10.1103/PhysRevLett.58.1490)
- Hopkins, A. M. 2018, *PASA*, 35, e039, doi: [10.1017/pasa.2018.29](https://doi.org/10.1017/pasa.2018.29)
- Hopkins, A. M., & Beacom, J. F. 2006, *ApJ*, 651, 142, doi: [10.1086/506610](https://doi.org/10.1086/506610)
- Horiuchi, S., Beacom, J. F., & Dwek, E. 2009, *PhRvD*, 79, 083013, doi: [10.1103/PhysRevD.79.083013](https://doi.org/10.1103/PhysRevD.79.083013)
- Horiuchi, S., Kinugawa, T., Takiwaki, T., Takahashi, K., & Kotake, K. 2021, *PhRvD*, 103, 043003, doi: [10.1103/PhysRevD.103.043003](https://doi.org/10.1103/PhysRevD.103.043003)
- Horiuchi, S., Sumiyoshi, K., Nakamura, K., et al. 2018, *MNRAS*, 475, 1363, doi: [10.1093/mnras/stx3271](https://doi.org/10.1093/mnras/stx3271)
- Iocco, F., Mangano, G., Miele, G., Raffelt, G. G., & Serpico, P. D. 2005, *Astroparticle Physics*, 23, 303, doi: [10.1016/j.astropartphys.2005.01.004](https://doi.org/10.1016/j.astropartphys.2005.01.004)
- Iv  n  ez-Ballesteros, P., & Volpe, M. C. 2023, *PhRvD*, 107, 023017, doi: [10.1103/PhysRevD.107.023017](https://doi.org/10.1103/PhysRevD.107.023017)
- Iwamoto, K., Mazzali, P. A., Nomoto, K., et al. 1998, *Nature*, 395, 672, doi: [10.1038/27155](https://doi.org/10.1038/27155)
- Kaplinghat, M., Steigman, G., & Walker, T. P. 2000, *PhRvD*, 62, 043001, doi: [10.1103/PhysRevD.62.043001](https://doi.org/10.1103/PhysRevD.62.043001)
- Kashiwagi, Y., Abe, K., Bronner, C., et al. 2024, *arXiv e-prints*, arXiv:2403.06760, doi: [10.48550/arXiv.2403.06760](https://doi.org/10.48550/arXiv.2403.06760)
- Kobayashi, C., Karakas, A. I., & Lugaro, M. 2020, *ApJ*, 900, 179, doi: [10.3847/1538-4357/abae65](https://doi.org/10.3847/1538-4357/abae65)
- Kobayashi, C., Umeda, H., Nomoto, K., Tominaga, N., & Ohkubo, T. 2006, *ApJ*, 653, 1145, doi: [10.1086/508914](https://doi.org/10.1086/508914)
- Krauss, L. M., Glashow, S. L., & Schramm, D. N. 1984, *Nature*, 310, 191, doi: [10.1038/310191a0](https://doi.org/10.1038/310191a0)
- Kresse, D., Ertl, T., & Janka, H.-T. 2021, *ApJ*, 909, 169, doi: [10.3847/1538-4357/abd54e](https://doi.org/10.3847/1538-4357/abd54e)
- Li, Y.-F., Vagins, M., & Wurm, M. 2022, *Universe*, 8, 181, doi: [10.3390/universe8030181](https://doi.org/10.3390/universe8030181)
- Lunardini, C. 2009, *PhRvL*, 102, 231101, doi: [10.1103/PhysRevLett.102.231101](https://doi.org/10.1103/PhysRevLett.102.231101)
- . 2016, *Astroparticle Physics*, 79, 49, doi: [10.1016/j.astropartphys.2016.02.005](https://doi.org/10.1016/j.astropartphys.2016.02.005)
- Madau, P., & Dickinson, M. 2014, *ARA&A*, 52, 415, doi: [10.1146/annurev-astro-081811-125615](https://doi.org/10.1146/annurev-astro-081811-125615)
- Malaney, R. A. 1997, *Astroparticle Physics*, 7, 125, doi: [10.1016/S0927-6505\(97\)00012-1](https://doi.org/10.1016/S0927-6505(97)00012-1)
- Mathews, G. J., Boccioli, L., Hidaka, J., & Kajino, T. 2020, *Modern Physics Letters A*, 35, 2030011, doi: [10.1142/S0217732320300116](https://doi.org/10.1142/S0217732320300116)
- Mathews, G. J., Hidaka, J., Kajino, T., & Suzuki, J. 2014, *ApJ*, 790, 115, doi: [10.1088/0004-637X/790/2/115](https://doi.org/10.1088/0004-637X/790/2/115)
- Mikheyev, S. P., & Smirnov, A. Y. 1985, *Yadernaya Fizika*, 42, 1441
- M  ller, K., Suliga, A. M., Tamborra, I., & Denton, P. B. 2018, *JCAP*, 2018, 066, doi: [10.1088/1475-7516/2018/05/066](https://doi.org/10.1088/1475-7516/2018/05/066)
- Nagakura, H., & Vartanyan, D. 2022, *MNRAS*, 512, 2806, doi: [10.1093/mnras/stac383](https://doi.org/10.1093/mnras/stac383)
- Nakazato, K. 2013, *PhRvD*, 88, 083012, doi: [10.1103/PhysRevD.88.083012](https://doi.org/10.1103/PhysRevD.88.083012)
- Nakazato, K., Mochida, E., Niino, Y., & Suzuki, H. 2015, *ApJ*, 804, 75, doi: [10.1088/0004-637X/804/1/75](https://doi.org/10.1088/0004-637X/804/1/75)
- Nakazato, K., Sumiyoshi, K., Suzuki, H., et al. 2013, *ApJS*, 205, 2, doi: [10.1088/0067-0049/205/1/2](https://doi.org/10.1088/0067-0049/205/1/2)
- Nakazato, K., Sumiyoshi, K., & Togashi, H. 2021, *PASJ*, 73, 639, doi: [10.1093/pasj/psab026](https://doi.org/10.1093/pasj/psab026)
- Nakazato, K., Sumiyoshi, K., & Yamada, S. 2006, *ApJ*, 645, 519, doi: [10.1086/504282](https://doi.org/10.1086/504282)
- Nomoto, K., Kobayashi, C., & Tominaga, N. 2013, *ARA&A*, 51, 457, doi: [10.1146/annurev-astro-082812-140956](https://doi.org/10.1146/annurev-astro-082812-140956)
- Nomoto, K., Tominaga, N., Umeda, H., Kobayashi, C., & Maeda, K. 2006, *NuPhA*, 777, 424, doi: [10.1016/j.nuclphysa.2006.05.008](https://doi.org/10.1016/j.nuclphysa.2006.05.008)
- Pignatari, M., Trueman, T. C. L., Womack, K. A., et al. 2023, *MNRAS*, 524, 6295, doi: [10.1093/mnras/stad2167](https://doi.org/10.1093/mnras/stad2167)
- Placco, V. M., Frebel, A., Beers, T. C., & Stancliffe, R. J. 2014, *ApJ*, 797, 21, doi: [10.1088/0004-637X/797/1/21](https://doi.org/10.1088/0004-637X/797/1/21)
- Poutanen, J., Lipunova, G., Fabrika, S., Butkevich, A. G., & Abolmasov, P. 2007, *MNRAS*, 377, 1187, doi: [10.1111/j.1365-2966.2007.11668.x](https://doi.org/10.1111/j.1365-2966.2007.11668.x)
- Priya, A., & Lunardini, C. 2017, *JCAP*, 2017, 031, doi: [10.1088/1475-7516/2017/11/031](https://doi.org/10.1088/1475-7516/2017/11/031)
- Sasaki, H., Yamazaki, Y., Kajino, T., et al. 2022, *ApJ*, 924, 29, doi: [10.3847/1538-4357/ac34f8](https://doi.org/10.3847/1538-4357/ac34f8)
- Sawatzki, J., Wurm, M., & Kresse, D. 2021, *PhRvD*, 103, 023021, doi: [10.1103/PhysRevD.103.023021](https://doi.org/10.1103/PhysRevD.103.023021)

- Schilbach, T. S. H., Caballero, O. L., & McLaughlin, G. C. 2019, *PhRvD*, 100, 043008, doi: [10.1103/PhysRevD.100.043008](https://doi.org/10.1103/PhysRevD.100.043008)
- Smartt, S. J. 2009, *ARA&A*, 47, 63, doi: [10.1146/annurev-astro-082708-101737](https://doi.org/10.1146/annurev-astro-082708-101737)
- . 2015, *PASA*, 32, e016, doi: [10.1017/pasa.2015.17](https://doi.org/10.1017/pasa.2015.17)
- Strigari, L. E., Beacom, J. F., Walker, T. P., & Zhang, P. 2005, *JCAP*, 2005, 017, doi: [10.1088/1475-7516/2005/04/017](https://doi.org/10.1088/1475-7516/2005/04/017)
- Strumia, A., & Vissani, F. 2003, *Physics Letters B*, 564, 42, doi: [10.1016/S0370-2693\(03\)00616-6](https://doi.org/10.1016/S0370-2693(03)00616-6)
- Sukhbold, T., Ertl, T., Woosley, S. E., Brown, J. M., & Janka, H. T. 2016, *ApJ*, 821, 38, doi: [10.3847/0004-637X/821/1/38](https://doi.org/10.3847/0004-637X/821/1/38)
- Suliga, A. M., Beacom, J. F., & Tamborra, I. 2022, *PhRvD*, 105, 043008, doi: [10.1103/PhysRevD.105.043008](https://doi.org/10.1103/PhysRevD.105.043008)
- Sumiyoshi, K., Furusawa, S., Nagakura, H., et al. 2023, *Progress of Theoretical and Experimental Physics*, 2023, 013E02, doi: [10.1093/ptep/ptac167](https://doi.org/10.1093/ptep/ptac167)
- Suwa, Y., Harada, A., Harada, M., et al. 2022, *ApJ*, 934, 15, doi: [10.3847/1538-4357/ac795e](https://doi.org/10.3847/1538-4357/ac795e)
- Suwa, Y., Harada, A., Mori, M., et al. 2024, arXiv e-prints, arXiv:2404.18248, doi: [10.48550/arXiv.2404.18248](https://doi.org/10.48550/arXiv.2404.18248)
- Suzuki, H. 1994, in *Physics and Astrophysics of Neutrinos*, XIII, ed. M. Fukugita & A. Suzuki, 420
- Tabrizi, Z., & Horiuchi, S. 2021, *JCAP*, 2021, 011, doi: [10.1088/1475-7516/2021/05/011](https://doi.org/10.1088/1475-7516/2021/05/011)
- Tano, T., Horai, T., Ashida, Y., et al. 2024, arXiv e-prints, arXiv:2405.15366, doi: [10.48550/arXiv.2405.15366](https://doi.org/10.48550/arXiv.2405.15366)
- Togashi, H., Nakazato, K., Takehara, Y., et al. 2017, *NuPhA*, 961, 78, doi: [10.1016/j.nuclphysa.2017.02.010](https://doi.org/10.1016/j.nuclphysa.2017.02.010)
- Totani, T., & Sato, K. 1995, *Astroparticle Physics*, 3, 367, doi: [10.1016/0927-6505\(95\)00015-9](https://doi.org/10.1016/0927-6505(95)00015-9)
- Totani, T., Sato, K., & Yoshii, Y. 1996, *ApJ*, 460, 303, doi: [10.1086/176970](https://doi.org/10.1086/176970)
- Tsujimoto, T. 2023, *MNRAS*, 518, 3475, doi: [10.1093/mnras/stac3351](https://doi.org/10.1093/mnras/stac3351)
- Vergani, S. D., Salvaterra, R., Japelj, J., et al. 2015, *A&A*, 581, A102, doi: [10.1051/0004-6361/201425013](https://doi.org/10.1051/0004-6361/201425013)
- Wei, Y.-F., Liu, T., & Song, C.-Y. 2024, *ApJ*, 966, 101, doi: [10.3847/1538-4357/ad3824](https://doi.org/10.3847/1538-4357/ad3824)
- Wolfenstein, L. 1978, *PhRvD*, 17, 2369, doi: [10.1103/PhysRevD.17.2369](https://doi.org/10.1103/PhysRevD.17.2369)
- Woosley, S. E., & Heger, A. 2006, *ApJ*, 637, 914, doi: [10.1086/498500](https://doi.org/10.1086/498500)
- Workman, R. L., Burkert, V. D., Crede, V., et al. 2022, *Progress of Theoretical and Experimental Physics*, 2022, 083C01, doi: [10.1093/ptep/ptac097](https://doi.org/10.1093/ptep/ptac097)
- Zhang, H., Abe, K., Hayato, Y., et al. 2015, *Astroparticle Physics*, 60, 41, doi: [10.1016/j.astropartphys.2014.05.004](https://doi.org/10.1016/j.astropartphys.2014.05.004)
- Ziegler, J. J., Edwards, T. D. P., Suliga, A. M., et al. 2022, *MNRAS*, 517, 2471, doi: [10.1093/mnras/stac2748](https://doi.org/10.1093/mnras/stac2748)